electronics

MDPI

Article

Band Alignment of AlN/InGaZnO Heterojunction for Thin-Film Transistor Application

Hongpeng Zhang [1,*], Tianli Huang [1], Rongjun Cao [1], Chen Wang [1], Bo Peng [2], Jibao Wu [3], Shaochong Wang [1], Kunwei Zheng [1], Renxu Jia [2], Yuming Zhang [2] and Hongyi Zhang [1]

[1] School of Opto-Electronic and Communication Engineering, Xiamen University of Technology, Xiamen 361024, China; 2322111010@stu.xmut.edu.cn (T.H.); 2222031224@s.xmut.edu.cn (R.C.); chenwang@xmut.edu.cn (C.W.); bcqh123001@outlook.com (S.W.); 2022000107@xmut.edu.cn (K.Z.); zhanghongyi@xmut.edu.cn (H.Z.)

[2] The Key Laboratory of Wide Band Gap Semiconductor Materials and Devices, School of Microelectronics, Xidian University, Xi'an 710071, China; boopeng@xidian.edu.cn (B.P.); rxjia@mail.xidian.edu.cn (R.J.); zhangym@xidian.edu.cn (Y.Z.)

[3] School of Mathematical Information, Shaoxing University, Shaoxing 312000, China; jbwu1015@usx.edu.cn

* Correspondence: hpzhang@xmut.edu.cn; Tel.: +86-157-7171-8620

Abstract: Uncrystallized indium-gallium-zinc-oxide (InGaZnO) thin-film transistors (TFTs) combined with an aluminum nitride (AlN) dielectric have been used to promote performance and steadiness. However, the high deposition temperature of AlN films limits their application in InGaZnO flexible TFTs. In this work, AlN layers were deposited via low-temperature plasma-enhanced atomic layer deposition (PEALD), and InGaZnO films were fabricated via high-power impulse magnetron sputtering (HIPIMS). The band alignment of the AlN/InGaZnO heterojunction was studied using the X-ray photoemission spectrum and ultraviolet visible transmittance spectrum. It was found that the AlN/InGaZnO system exhibited a staggered band alignment with a valence band offset ΔE_v of -1.25 ± 0.05 eV and a conduction band offset ΔE_c of 4.01 ± 0.05 eV. The results imply that PEALD AlN could be more useful for surface passivation than a gate dielectric to promote InGaZnO device reliability under atmospheric exposure.

Keywords: indium-gallium-zinc-oxide; band offset; X-ray photoelectron spectroscopy; aluminum nitride; high-power impulse magnetron sputtering (HIPIMS)

Citation: Zhang, H.; Huang, T.; Cao, R.; Wang, C.; Peng, B.; Wu, J.; Wang, S.; Zheng, K.; Jia, R.; Zhang, Y.; et al. Band Alignment of AlN/InGaZnO Heterojunction for Thin-Film Transistor Application. *Electronics* **2024**, *13*, 4602. https://doi.org/10.3390/electronics13234602

Academic Editor: Esteban Tlelo-Cuautle

Received: 22 October 2024
Revised: 15 November 2024
Accepted: 20 November 2024
Published: 22 November 2024

1. Introduction

Indium-gallium-zinc-oxide (InGaZnO, or IGZO) has been deemed as one of the promising channel candidates for flexible thin-film transistors (TFTs) due to its high mobility, excellent optical transparency, and the capacity to grow on flexible substrates at low temperatures with decent quality [1–3]. Meanwhile, IGZO FETs have also made impressive progress in emerging technologies, such as flat planer displays [2], flexible circuits [4,5], and electronic paper [6]. In spite of the great number of studies on InGaZnO TFTs, their low operation voltage and long-term reliability are issues that still need to be explored [7–10]. These issues have been attributed to the charge trapping at IGZO/dielectric interface or the conductivity modifications of the IGZO channel due to the exposure to the hydrogen or water in the atmosphere [7–10]. The high-k gate dielectric was one of the effective solutions for reducing the threshold voltage and subthreshold swing, which promote capacitance coupling at the IGZO/dielectric interface [3,8]. However, the small bandgap (E_g) of the high-k dielectric results in an insufficient band offset (ΔE) at the InGaZnO/dielectric interface, which is unable to prevent the injection of electrons and holes [10–12]. There are many reported studies on the band alignments between InGaZnO and insulators, such as SiO_2 [13], Al_2O_3 [14], HfO_2 [15], HfSiO [11], HfTiO [16], HfLaO [17], $ZrSiO_x$ [18], and Sc_2O_3 [8]. Even if a specific dielectric is unsuitable for the gate of IGZO TFTs, it may

play role in surface passivation, which is vital for IGZO TFTs due to their reliability being hindered by exposure to the hydrogen or water in the atmosphere [10,19].

To the dielectrics mentioned above, aluminum nitride (AlN) is a viable alternative solution due to its high dielectric constant (~9.5 [20]) and E_g (~6.2 eV) [21], superior thermal conductivity of ~17 $W \cdot m^{-1}K^{-1}$ [22], low thermal expansion coefficient (~5.3 $\times$ 10^{-6} K^{-1} [23]), and suitable thermal stability [24]. InGaZnO TFTs using AlN have been reported and achieved acceptable device performance with a reduced self-heating effect [25,26]. However, to the best of our knowledge, no study has been conducted on the band offsets in the AlN/InGaZnO heterojunction. In this work, by using X-ray photoelectron spectroscopy, the band offsets in the InGaZnO/AlN heterojunction were analyzed, and InGaZnO and AlN film were fabricated by high-power impulse magnetron sputtering (HIPIMS) and plasma-enhanced atomic layer deposition (PEALD), respectively.

2. Materials and Methods

2.1. Fabrication of Samples

The InGaZnO films were prepared with a physical vapor deposition system (Ljuhv SP122I, Jhubei city, Taiwan, China). The system at our institute has been used to deposit TCO films such as IGZO and ITO in previous studies [7,27–29]. In this work, InGaZnO was deposited by HIPIMS on c-plane sapphire wafers (α-Al_2O_3 (0001)) and quartz substrates based in a ceramic target of InGaZnO (99.99% purity, In_2O_3:Ga_2O_3:ZnO = 1:1:1). The radio frequency (RF) power and operating pressure were, respectively, 50 W and 40 mTorr, in a pure Ar ambient environment. Further deposition details of InGaZnO can be found in a previous work [7]. Prior to deposition, the wafers were divided into 10 mm $\times$ 10 mm pieces, which were ultrasonically washed with normal organic cleaners (acetone, isopropanol, and ultrapure water for 10 min each). HIPIMS-InGaZnO films exhibited an amorphous state according to X-ray diffraction [7]. For uncrystallized InGaZnO films, high-temperature deposition or annealing are improper because InGaZnO is widely used for low-temperature applications with wafers like plastic and tape [7].

In this work, a Beneq TFS-200 reactor and the PEALD technique were utilized to grow AlN at 185 °C. Given the requirements for a flexible thin-film transistor as well as the AlN film quality, a low deposition temperature was used in this work, which has been reported in the literature [30]. The precursors were trimethylaluminum (TMA) and ammonia (NH_3), using Al and N sources, respectively. Further AlN deposition details can be found in the literature [30]. In this work, three samples (1#–3#) were used for XPS experiments: (1) 100 nm-thick IGZO on sapphire; (2) 3 nm-thick AlN grown on IGZO; (3) 40 nm-thick AlN grown on IGZO.

2.2. Characterizations

A mature method [31] was used to calculate the valence band offset (ΔE_c) and conduction band offset (ΔE_v) based in X-ray photoelectron spectroscopy (XPS) [3,8,17,18,21,31]. A Thermo ESCALAB 250 X-ray photoelectron spectrometer with a monochromatic Al -Kα X-ray source (energy 1486.6 eV) was used for ex situ XPS measurements. The X-ray source possessed a power of 300W, and the detection region was set was a spot with a radius of 650 µm and a take-off angle of 90°. XPS survey scans with 1.0 eV/step were used to detect the chemical state of samples 1–3#. High resolution scans with 0.05 eV/step and pass energy of 30 eV were utilized to evaluate the binding energy of specific elements. In addition, the valence band scans shared the same settings as the high-resolution scans. It should be noted that the whole XPS spectra were corrected using the C 1s peak (using ~284.8 eV), which stems from surface carbon contamination to compensate for the charging effect [3]. A 30 s Ar ion sputtering was used for sample 3#, which was followed immediately by XPS measurements to eliminate the potential influence coming from the atmosphere, water vapor, etc. The surface micromorphologies of the fabricated films were detected with a Bruker Dimension Icon atomic force microscope (AFM). The E_g of AlN was evaluated using

the sample fabricated on quartz using the UV–visible transmittance spectrum (JASCO, wavelength range of 180–600 nm).

3. Results and Discussion

3.1. Chemical Bonding State Analysis

XPS survey scans with an 89.45 eV pass energy were obtained to analyze the different chemical composition states in the InGaZnO, 3 nm AlN on InGaZnO, and 40 nm AlN films. The O 1s, Ga 2p, C 1s, Zn 2p, N 1s, Al 2p, In 3p, In 3d, and In 4d peaks were seen in the survey spectra of samples 1#–3# (Figure 1), which originated from In, Zn, Ga, Al, C, and O. Table 1 provides the atomic ratios of the different elements in the targets and samples 1# and 3#. Specifically, for the HIPIMS InGaZnO films, the Ga ratio and Zn ratio were higher than those in the target materials, and the In ratio and O ratio were lower than those in the target materials, which is similar with reported HIPIMS InGaZnO films [6].

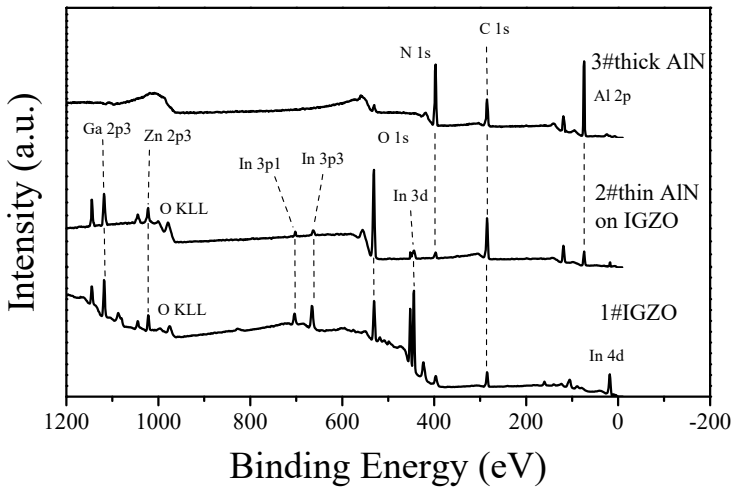

Figure 1. XPS survey scans of samples 1#–3# (IGZO, thin AlN, thick AlN).

Table 1. Relative atomic ratios of the specific elements in IGZO targets, samples 1# and 3#.

Sample	In (%)	Zn (%)	Ga (%)	O (%)	Al (%)	N (%)
IGZO Target	16.67	8.33	16.67	58.33	NR	NR
1#	14.34	12.44	17.11	48.67	7.44	NR
3#	NR	NR	NR	1.63	51.15	47.22

Firstly, the high Zn ratio could be attributed to the much larger sputtering yield (Zn: 3.68 [6]), which accelerated the Zn sputtering off from the target to the substrate surface and increased the Zn percentage in the InGaZnO films. Secondly, compared with Ga, In experienced more collision scattering during sputtering due to its longer mean free path [6]. In addition, the actual Al: N ratio of sample 3# (~1.08:1) was different from the ideal ratio (1:1). It may have resulted from the high hygroscopicity of Al_2O_3 (Al-O) and sample 3# being exposed to atmospheric water vapor or hydrogen before the XPS measurements. In addition, the surface morphology of InGaZnO and AlN is shown in Figure 2. Both the InGaZnO and AlN films had a flat surface with a relatively low root mean square (RMS) roughness of 1.02 and 0.32 nm, respectively. A flat surface is beneficial for suppressing surface recombination and leakage current, which thus increase the performance of IGZO TFT devices.

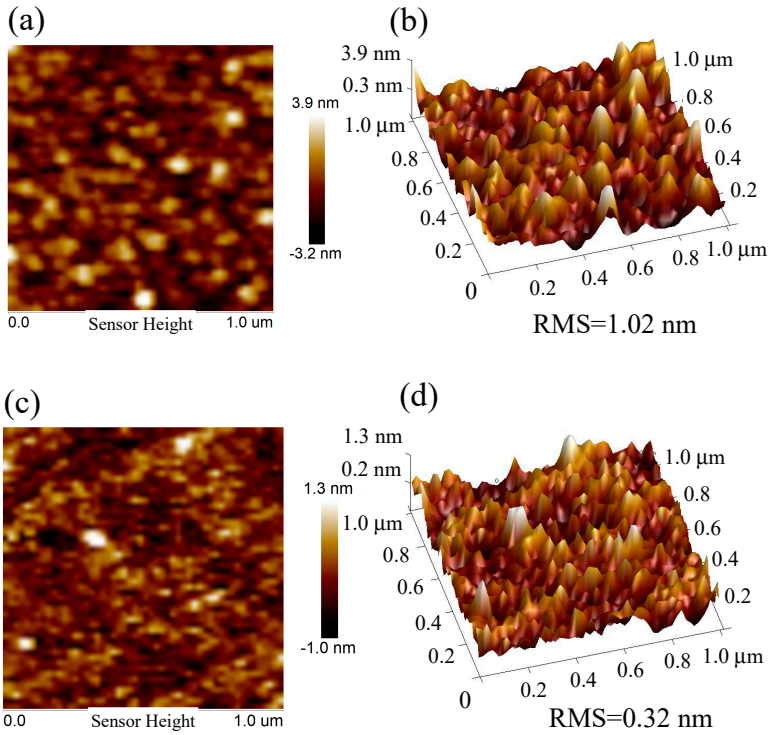

Figure 2. The 2D and 3D AFM plots of InGaZnO (**a**,**b**), AlN films (**c**,**d**).

3.2. Energy Gap of AlN, IGZO

The E_g of the InGaZnO and AlN was, respectively, evaluated using the XPS O 1s CL spectrum and ultraviolet-to-visible transmittance spectrum. According to the O 1s spectra in Figure 3, the E_g of InGaZnO and AlN was 3.42 and 6.18 ± 0.05 eV, respectively. As shown in Figure 3a, the energy loss structure on the high- energy side was used to evaluate the E_g of the InGaZnO films [32,33]. The measured value for IGZO is in agreement with the reported values (~3.4–3.6 eV) [3,34,35] but is higher than in some reports (~3.2 eV) [8,18]. In addition, the E_g of the direct bandgap semiconductor AlN was extracted from the Tauc plot ($(\alpha h\nu)^2$ vs. $h\nu$) based on the UV–visible transmittance spectrum, which is close to the reported values (~6.2 eV [20,21,36–38]).

3.3. Band Alignment Analysis

Figure 4 shows the valence band spectra for the thick InGaZnO and AlN films, and the valence band maximum (VBM) of InGaZnO and AlN is obtained (2.32 and 1.73 ± 0.05 eV, respectively). The VBM values were extracted by linear extrapolation [8,16–18] based on Figure 4, and the values are similar to those reported for sputtered InGaZnO [8,16–18] and ALD AlN films [21,30].

Using the evaluation method proposed by Kraut et al. [31], the valence band offset (ΔE_v) of the AlN/InGaZnO heterojunction can be calculated as

$$\Delta E_v = (E_{Core} - E_{VBM})_{InGaZnO} - (E_{Core} - E_{VBM})_{AlN} - (E_{Core}^{InGaZnO} - E_{Core}^{AlN})_{AlN/InGaZnO} \quad (1)$$

where E_{core} and E_{VBM} are, respectively, the core level (CL) positions and the VBM of these bulk materials, combined with the CL difference of the thin AlN/InGaZnO film.

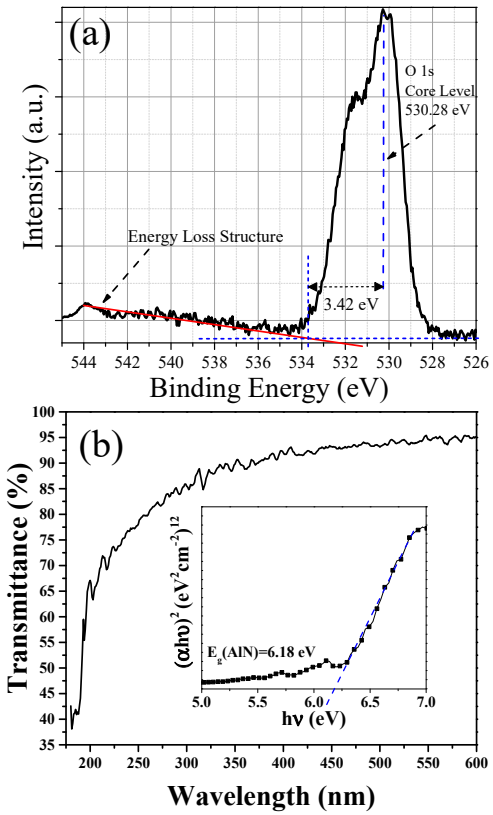

Figure 3. O *1s* core-level binding energy spectrum of (**a**) InGaZnO with energy loss structure, (**b**) the UV–visible transmittance spectrum and corresponding Tauc plot ($(\alpha h\nu)^2$ vs. hν) of AlN.

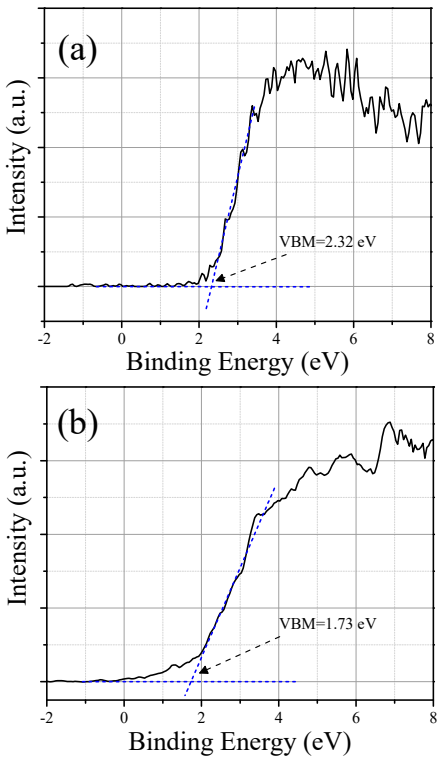

Figure 4. Valence band (VB) spectra for (**a**) InGaZnO and (**b**) thick AlN.

According to Kraut's method, we further measured the core-level spectra of samples 1#–3# to evaluate the actual band alignment and the corresponding band offsets (ΔE_v and ΔE_c). The high-resolution core-level spectra are provided in Figure 5 for (a) InGaZnO VBM with CLs and (b) AlN VBM with CLs, as well as in Figure 6 for the InGaZnO-AlN CLs. Figures 5 and 6 were utilized to evaluate the specific CL peak positions. Table 2 exhibits the extracted values; thus, the valence band offset ΔE_v with different CLs (Zn, Ga, O) were calculated as −1.28, −1.19, and −1.28 ± 0.05 eV, respectively. The average ΔE_v of AlN/InGaZnO was calculated as nearly −1.25 eV.

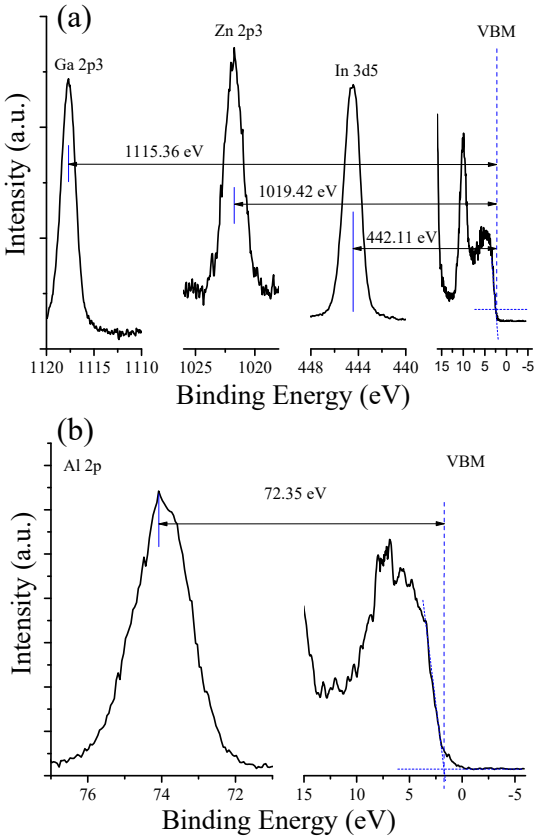

Figure 5. XPS CL and VB spectra for (**a**) thick InGaZnO VBM-CL sample, and (**b**) thick AlN VBM-CL sample.

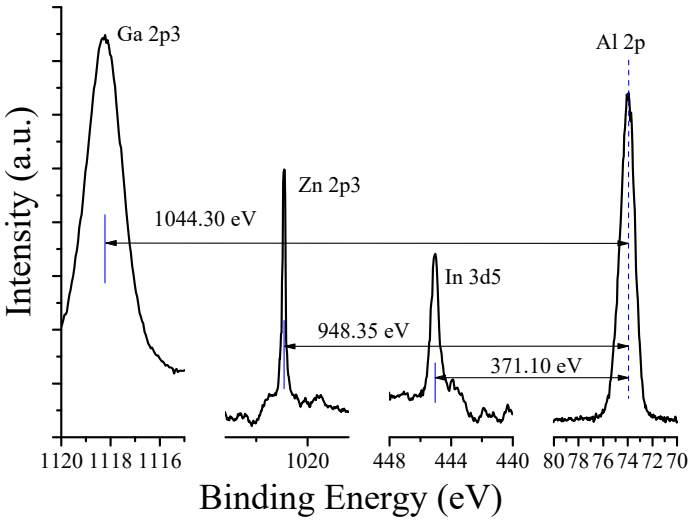

Figure 6. High-resolution XPS spectra for InGaZnO and AlN CLs.

Table 2. Summary of XPS data on IGZO, AlN, and AlN/IGZO samples. Peak position values and VBM values are ± 0.05 eV.

IGZO Metal Core	1# Thick IGZO Metal Core Level	1# Thick IGZO Metal Core-IGZO VBM	3# Thick AlN Al 2p Core Level	2# Thin AlN on IGZO Al2p-AlN VBM	2# Thin AlN on IGZO ΔCL IGZO-AlN	Valence Band Offset	Average ΔE_v	Conduction Band Offset
Zn2p3	1021.74	1019.42	74.08	72.35	948.35	−1.28	−1.25	4.04
Ga2p3	1117.68	1115.36			1044.30	−1.19		3.95
In3d5	444.49	442.17			371.10	−1.28		4.04

Subsequently, the conduction band offset ΔE_c of AlN/IGZO was calculated to be 3.86, 3.87, and 3.92 ± 0.05 eV with different CLs (Zn, Ga, O) using the following equation [3,9–14]:

$$\Delta E_c = E_g(AlN) - E_g(IGZO) - \Delta E_v \quad (2)$$

Figure 7 exhibits the abbreviated band diagram and the complete band diagram of the AlN/InGaZnO heterojunction. These results demonstrate that a staggered alignment (or type-II) existed at the AlN/InGaZnO heterojunction with an average ΔE_v of −1.25 ± 0.05 eV and an average ΔE_c of 4.01 ± 0.05 eV. The PEALD AlN film had a large E_g and ΔE_c but a negative ΔE_v, which could provide sufficient electron confinement combined with undesirable hole confinement. These results imply that the PEALD AlN is not the perfect candidate as a gate dielectric in InGaZnO TFTs because of the inability to confine holes may result in serious device instability issues owing to the various hole defects or acceptor traps. Additionally, AlN still plays a vital role in the surface passivation of InGaZnO devices, which promotes device stability during atmospheric exposure [11,12].

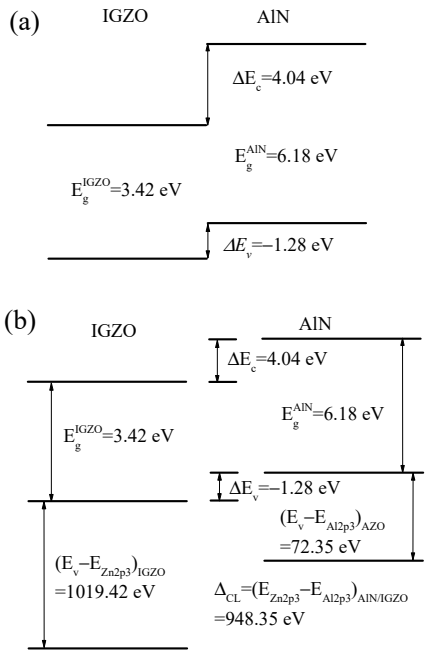

Figure 7. (**a**) The simplified and (**b**) detailed band diagrams of the AlN/IGZO heterojunction.

4. Conclusions

The AlN/InGaZnO heterojunction was found to have a staggered alignment. AlN and InGaZnO were, respectively, produced via PEALD and HIPIMS. The corresponding ΔE_c and ΔE_v were evaluated to be 4.01 ± 0.05 eV and −1.25 ± 0.05 eV, respectively. These results suggest that AlN could provide a sufficient barrier for electrons but cannot

hinder holes on InGaZnO, which form the threshold voltage and cause the long-term instability of InGaZnO TFTs. In addition, they indicate that AlN is more suitable for surface passivation to prevent InGaZnO surfaces from exposure to atmosphere hydrogen and oxygen. This accurate determination provides useful information for the further development of transparent TFTs.

Author Contributions: H.Z. (Hongpeng Zhang): conceptualization, methodology, writing—original draft, supervision, funding acquisition. T.H.: writing sample original draft, validation, investigation, formal analysis, data curation. R.C.: investigation, data curation. C.W.: resources. B.P.: validation, funding acquisition, formal analysis. J.W.: investigation, data curation. S.W.: investigation, data curation. K.Z.: formal analysis. R.J.: conceptualization, resources. Y.Z.: formal analysis. H.Z. (Hongyi Zhang): supervision, formal analysis. All authors have read and agreed to the published version of the manuscript.

Funding: This research was funded by the National Natural Science Foundation of China (62004153); Natural Science Foundation of Xiamen, China (3502Z20227070); the Youth Innovation Fund of Xiamen, China (3502Z20206074); Xiamen major science and technology projects (3502Z20221022); the Scientific project of Xiamen University of Technology (YKJ22049R).

Data Availability Statement: Data will be made available upon request.

Conflicts of Interest: The authors declare that they have no known competing financial interests or personal relationships that could have appeared to influence the work reported in this paper.

References

1. Nomura, K.; Ohta, H.; Ueda, K.; Kamiya, T.; Hirano, M.; Hosono, H. Thin-film transistor fabricated in single-crystalline transparent oxide semiconductor. *Science* **2003**, *300*, 1269–1272. [CrossRef] [PubMed]
2. Nomura, K.; Ohta, H.; Takagi, A.; Kamiya, T.; Hirano, M.; Hosono, H. Room temperature fabrication of transparent flexible thin-film transistors using amorphous oxide semiconductors. *Nature* **2004**, *432*, 488–492. [CrossRef] [PubMed]
3. Hays, D.C.; Gila, B.P.; Pearton, S.J.; Ren, F. Energy band offsets of dielectrics on $InGaZnO_4$. *Appl. Phys. Rev.* **2017**, *4*, 021301. [CrossRef]
4. Honda, W.; Arie, T.; Akita, S.; Takei, K. Mechanically Flexible and High-Performance CMOS Logic Circuits. *Sci. Rep.* **2015**, *5*, 15099. [CrossRef]
5. Kamiya, T.; Nomura K and Hosono, H. Present status of amorphous In–Ga–Zn–O thin-film transistors. *Sci. Technol. Adv. Mater.* **2010**, *11*, 044305. [CrossRef]
6. Lim, W.; Douglas, E.A.; Kim, S.H.; Norton, D.P.; Pearton, S.J.; Ren, F.; Shen, H.; Chang, W.H. High mobility $InGaZnO_4$ thin-film transistors on paper. *Appl. Phys. Lett.* **2009**, *94*, 072103. [CrossRef]
7. Zhao, M.; Chen, Z.; Shi, C.; Chen, Q.; Xu, M.; Wu, W.; Wu, D.; Lien, S.; Zhu, W. Modulation of carrier density in indium–gallium–zinc-oxide thin film prepared by high-power impulse magnetron sputtering. *Vacuum* **2023**, *207*, 111640. [CrossRef]
8. Hays, D.C.; Gila, B.P.; Pearton, S.J.; Thorpe, R.; Ren, F. Band offsets in sputtered $Sc_2O_3/InGaZnO_4$ heterojunctions. *Vacuum* **2017**, *136*, 137–141. [CrossRef]
9. Bai, Z.; Lu, N.; Wang, J.; Geng, D.; Liu, D.; Xiao, K.; Li, L. A novel extraction method of device parameters for thin-film transistors (TFTs). *Phys. Lett.* **2021**, *403*, 127386. [CrossRef]
10. Nomura, K.; Kamiya, T.; Hosono, H. Stability and high-frequency operation of amorphous In–Ga–Zn–O thin-film transistors with various passivation layers. *Thin Solid Films* **2012**, *520*, 3778–3782. [CrossRef]
11. Hays, D.C.; Gila, B.P.; Pearton, S.J. Effect of deposition conditions and composition on band offsets in atomic layer deposited $Hf_xSi_{1-x}O_y$ on $InGaZnO_4$. *J. Vac. Sci. Technol. B* **2017**, *35*, 011206. [CrossRef]
12. Liu, P.; Chang, C.; Chang, C. Suppression of photo-bias induced instability for amorphous indium tungsten oxide thin film transistors with bi-layer structure. *Appl. Phys. Lett.* **2016**, *108*, 261602. [CrossRef]
13. Lee, J.; Park, J.S.; Pyo, Y.S.; Lee, D.B.; Kim, E.H.; Stryakhilev, D.; Kim, T.W.; Jin, D.U.; Mo, Y.G. The influence of the gate dielectrics on threshold voltage instability in amorphous indium-gallium-zinc oxide thin film transistors. *Appl. Phys. Lett.* **2009**, *95*, 123502. [CrossRef]
14. Lee, J.M.; Cho, I.; Lee, J.H.; Cheong, W.S.; Hwang, C.S.; Kwon, H.I. Comparative study of electrical instabilities in top-gate InGaZnO thin film transistors with Al_2O_3 and Al_2O_3/SiN_x gate dielectrics. *Appl. Phys. Lett.* **2009**, *94*, 222112. [CrossRef]
15. Chang, S.; Song, Y.W.; Lee, S.; Lee, S.Y.; Ju, B.K. Efficient suppression of charge trapping in ZnO-based transparent thin film transistors with novel $Al_2O_3/HfO_2/Al_2O_3$ structure. *Appl. Phys. Lett.* **2008**, *92*, 192104. [CrossRef]
16. He, G.; Chen, X.F.; Lv, J.G.; Fang, Z.B.; Liu, Y.M.; Zhu, K.R.; Sun, Z.Q.; Liu., M. Band offsets in $HfTiO/InGaZnO_4$ heterojunction determined by X-ray photoelectron spectroscopy. *J. Alloys Compd.* **2015**, *642*, 172–176. [CrossRef]

17. Qian, L.; Wu, Z.; Zhang, Y.; Liu, Y.; Song, J.; Liu, X.; Li, Y. Band alignment and interfacial chemical structure of the HfLaO/$InGaZnO_4$ heterojunction investigated by x-ray photoelectron spectroscopy. *J. Phys. D Appl. Phys.* **2017**, *50*, 145106. [CrossRef]
18. Hays, D.C.; Gila, B.P.; Pearton, S.J.; Ren, F. $ZrSiO_x$/IGZO heterojunctions band offsets determined by X-ray photoelectron spectroscopy. *Vacuum* **2015**, *122*, 195–200. [CrossRef]
19. Sung, S.Y.; Choi, J.H.; Han, U.B.; Lee, K.C.; Lee, J.H.; Kim, J.J.; Lim, W.; Pearton, S.J.; Norton, D.P.; Heo, Y.W. Effects of ambient atmosphere on the transfer characteristics and gate-bias stress stability of amorphous indium-gallium-zinc oxide thin-film transistors. *Appl. Phys. Lett.* **2010**, *96*, 102107. [CrossRef]
20. Yim, W.M.; Stofko, E.J.; Zanzucchi, P.J.; Pankove, J.I.; Ettenberg, M.; Gilbert, S.L. Epitaxially grown AlN and its optical band gap. *J. Appl. Phys.* **1973**, *44*, 292. [CrossRef]
21. Chen, J.; Tao, J.; Ma, H.; Zhang, H.; Feng, J.; Liu, W.; Xia, C.; Lu, H.; Zhang, D. Band alignment of AlN/β-Ga_2O_3 heterojunction interface measured by X-ray photoelectron spectroscopy. *Appl. Phys. Lett.* **2018**, *112*, 261602. [CrossRef]
22. Duquenne, C.; Besland, M.P.; Tessier, P.Y.; Gautron, E.; Scudeller, Y.; Averty, D. Thermal conductivity of aluminium nitride thin films prepared by reactive magnetron sputtering. *J. Phys. D Appl. Phys.* **2012**, *45*, 015301. [CrossRef]
23. Tungare, M.; Kamineni, V.K.; Shahedipour-Sandvik, F.; Diebold, A.C. Dielectric properties and thickness metrology of strain engineered GaN/AlN/Si (111) thin films grown by MOCVD. *Thin Solid Films* **2011**, *519*, 2929–2932. [CrossRef]
24. Gould, R.; Awan, S. Dielectric properties of AlN_x thin films prepared by RF magnetron sputtering of Al using a N_2/Ar sputtering gas mixture. *Thin Solid Films* **2004**, *469*, 184–189. [CrossRef]
25. Besleaga, C.; Stan, G.E.; Pintilie, I.; Barquinha, P.; Fortunato, E.; Martins, R. Transparent field-effect transistors based on AlN-gate dielectric and IGZO channel semiconductor. *Appl. Surf. Sci.* **2016**, *379*, 270. [CrossRef]
26. Kao, M.; Liang, Y.; Lin, Y.; Weng, Y.; Dee, C.; Liu, P.; Lee, C.; Chang, E. InGaZnO Ferroelectric Thin-Film Transistor Using HfO_2/Al_2O_3/AlN Hybrid Gate Dielectric Stack With Ultra-Large Memory Window. *IEEE Electron Device Lett.* **2022**, *43*, 2105–2108. [CrossRef]
27. Zhao, M.; Zhang, J.; Huang, Q.; Wu, W.; Tseng, M.; Lien, S.; Zhu, W. Effect of working pressure on Sn/In composition and optoelectronic properties of ITO films prepared by high power impulse magnetron sputtering. *Vacuum* **2022**, *196*, 110762. [CrossRef]
28. Zhao, M.; Zhang, J.; Huang, J.; Huang, Q.; Wu, W.; Tseng, M.; Huang, C.; Kuo, H.; Lien, S.; Zhu, W. Effect of power density on compositional and structural evolution of ITO thin film by HiPIMS method. *Vacuum* **2022**, *200*, 111034. [CrossRef]
29. Chen, H.; Hsu, C.; Wu, W.; Zhang, W.; Zhang, J.; Zhang, X.; Gao, P.; Wu, D.; Lai, F.; Lien, S.; et al. Substrate temperature effects on PEALD HfAlO dielectric films for IGZO-TFT applications. *Appl. Surf. Sci.* **2024**, *665*, 160305. [CrossRef]
30. Alevli, M.; Qzgit, C.; Donmez, I.; Biyikli, N. Structural properties of AlN films deposited by plasma-enhanced atomic layer deposition at different growth temperatures. *Phys. Status Solidi A* **2012**, *209*, 266–271. [CrossRef]
31. Kraut, E.A.; Grant, R.W.; Waldrop, J.R.; Kowalczyk, S.P. Precise determination of the valence-band edge in X-ray photoemission spectra: Application to measurement of semiconductor interface potentials. *Phys. Rev. Lett.* **1980**, *44*, 1620–1623. [CrossRef]
32. Kamimura, T.; Sasaki, K.; Wong, M.H.; Krishnamurthy, D.; Kuramata, A.; Masui, T.; Yamakoshi, S.; Higashiwaki, M. Band alignment and electrical properties of Al_2O_3/β-Ga_2O_3 heterojunctions. *Appl. Phys. Lett.* **2014**, *104*, 192104. [CrossRef]
33. Konishi, K.; Kamimura, T.; Wong, M.H.; Sasaki, K.; Kuramata, A.; Yamakoshi, S.; Higashiwaki, M. Large conduction band offset at SiO_2/β-Ga_2O_3 heterojunction determined by X-ray photoelectron spectroscopy. *Phys. Status Solidi B* **2016**, *253*, 623–625. [CrossRef]
34. Huan, Y.; Wang, X.; Liu, W.; Dong, H.; Long, S.; Sun, S.; Yang, J.; Wu, S.; Yu, W.; Horng, R.; et al. Band alignment of indium–gallium–zinc oxide/β-Ga_2O_3 (-201) heterojunction determined by angle-resolved X-ray photoelectron spectroscopy. *Jpn. J. Appl. Phys.* **2018**, *57*, 100312. [CrossRef]
35. Zheng, C.Y.; He, G.; Chen, X.F.; Liu, M.; Lv, J.G.; Gao, J.; Zhang, J.W.; Xiao, D.Q.; Jin, P.; Jiang, S.S.; et al. Modification of band alignments and optimization of electrical properties of InGaZnO MOS capacitors with high-k HfO_xN_y gate dielectrics. *J. Alloys Compd.* **2016**, *679*, 115–121. [CrossRef]
36. Thapa, R.; Saha, B.; Chattopadhyay, K.K. Enhanced field emission from Si doped nanocrystalline AlN thin films. *Appl. Surf. Sci.* **2009**, *255*, 4536. [CrossRef]
37. Dumitru, V.; Morosanu, C.; Sandu, V.; Stoica, A. Optical and structural differences between RF and DC Al_xN_y magnetron sputtered films. *Thin Solid Films* **2000**, *359*, 17–20. [CrossRef]
38. Fares, C.; Ren, F.; Tadjer, M.J.; Woodward, J.; Mastro, M.A.; Feigelson, B.N.; Eddy, C.R.; Pearton, S.J. Band offset determination for amorphous Al_2O_3 deposited on bulk AlN and atomic-layer epitaxial AlN on sapphire. *Appl. Phys. Lett.* **2020**, *117*, 182103. [CrossRef]